


Freestanding oxide membranes: synthesis, tunable physical properties, and functional devices

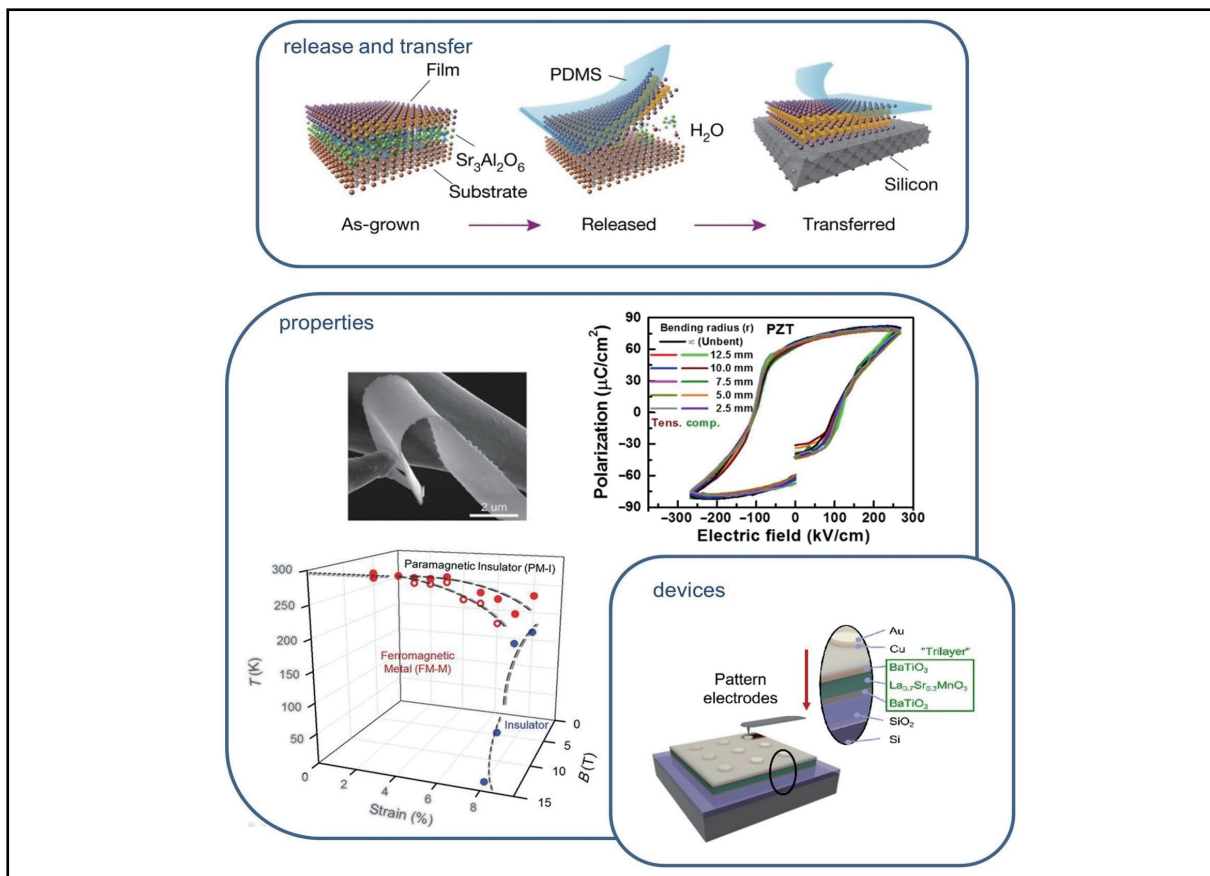
Ao Wang, Jinfeng Zhang , and Lingfei Wang 

Hefei National Research Center for Physical Sciences at Microscale, University of Science and Technology of China, Hefei 230026, China

 Correspondence: Jinfeng Zhang, E-mail: zjinfeng@mail.ustc.edu.cn; Lingfei Wang, E-mail: wanglf@ustc.edu.cn

© 2024 The Author(s). This is an open access article under the CC BY-NC-ND 4.0 license (<http://creativecommons.org/licenses/by-nc-nd/4.0/>).

Graphical abstract



Schematic for the preparation process of freestanding oxide films, along with examples of physical properties research and device applications.

Public summary

- The preparation methods of freestanding films, as well as the advantages and disadvantages of various methods, are summarized.
- The research on the properties and devices of freestanding oxide films is presented.
- This review provides insights into the future development of freestanding oxide films.

Freestanding oxide membranes: synthesis, tunable physical properties, and functional devices

Ao Wang, Jinfeng Zhang , and Lingfei Wang 

Hefei National Research Center for Physical Sciences at Microscale, University of Science and Technology of China, Hefei 230026, China

 Correspondence: Jinfeng Zhang, E-mail: zjinfeng@mail.ustc.edu.cn; Lingfei Wang, E-mail: wanglf@ustc.edu.cn

© 2024 The Author(s). This is an open access article under the CC BY-NC-ND 4.0 license (<http://creativecommons.org/licenses/by-nc-nd/4.0/>).



Cite This: *JUSTC*, 2024, 54(7): 0701 (16pp)



Read Online

Abstract: The study of oxide heteroepitaxy has been hindered by the issues of misfit strain and substrate clamping, which impede both the optimization of performance and the acquisition of a fundamental understanding of oxide systems. Recently, however, the development of freestanding oxide membranes has provided a plausible solution to these substrate limitations. Single-crystalline functional oxide films can be released from their substrates without incurring significant damage and can subsequently be transferred to any substrate of choice. This paper discusses recent advancements in the fabrication, adjustable physical properties, and various applications of freestanding oxide perovskite films. First, we present the primary strategies employed for the synthesis and transfer of these freestanding perovskite thin films. Second, we explore the main functionalities observed in freestanding perovskite oxide thin films, with special attention to the tunable functionalities and physical properties of these freestanding perovskite membranes under varying strain states. Next, we encapsulate three representative devices based on freestanding oxide films. Overall, this review highlights the potential of freestanding oxide films for the study of novel functionalities and flexible electronics.

Keywords: freestanding oxide membranes; transition metal oxides; thin films; electronic devices

CLC number: O469

Document code: A

1 Introduction

Transition metal oxides (TMOs), particularly ABO_3 perovskite materials, exhibit a broad range of functionalities, including high-temperature superconductivity^[1], metal-insulator transitions^[2], multiferroicity^[3], ionic conduction^[4], and colossal magnetoresistance^[5]. These diverse properties arise from the interaction of charge, spin, orbital, and lattice degrees of freedom. The strongly correlated nature of these degrees of freedom typically results in complex phase diagrams and high tunability under external stimuli^[6]. In light of the rapid development of state-of-the-art deposition tools, such as oxide molecular beam epitaxy, reflection high-energy electron diffraction (RHEED)-assisted pulsed laser deposition (PLD), and atomic layer deposition, it is now practical to routinely fabricate atomically perfect heterostructures of complex perovskites. This has led to a growing interest in oxide epitaxial films due to their emergent interfacial phenomena and superior functionalities^[7]. On this basis, flexible oxide films and membranes with high quality comparable to those of epitaxial films, if realized, should promote the development of electronic devices with high integration levels and wearability^[8–10].

With the rapid advancement of artificial intelligence and the emergence of a new generation of functional devices, oxide films with stable and tunable physical properties have become increasingly important^[11–13]. However, traditional epitaxial thin films are strictly bound to substrates, a restriction that limits their further application. On the one hand, the

elastic deformations induced in the films are limited to the planar strains induced by the epitaxy on the compatible substrates^[14]. On the other hand, the substrates usually have strong covalent and ionic bonds, which are unable to impart mechanical flexibility to the films. Additionally, the formation of strong chemical bonds at the interface can limit the functional response of the films when structural changes occur upon the application of external stimuli. These include piezoelectric/magnetostrictive deformations, ferroelastic domain motion during polarization switching in ferroelectrics^[15], or strain-mediated magnetoelectric effects in multiferroic heterostructures^[16]. Consequently, the release of epitaxial oxide films from their growth substrates represents a promising opportunity to expand our understanding of oxide films by studying their intrinsic responses in a two-dimensional (2D) isolated system and to explore new strategies for mechanical manipulation.

To address the above issue, many strategies have been employed in recent years. For instance, we can deposit single-crystalline films on layered materials such as mica and graphene^[17–19], or exfoliate freestanding thin films from hard substrates by using chemical or physical methods^[20–22]. The membranes can be transferred directly onto any substrate, thus bypassing the limitations of conventional epitaxy and presenting a new platform for investigating the fundamental properties of large regimes of strain and strain gradients^[23,24]. Moreover, depending on whether 2D films are used as freestanding monolayers or are stacked into bilayers or multilayers,

a wide variety of property phenomena arise, which can deviate significantly from the behavior of the bulk crystal, leading to a variety of different applications^[25]. In this review, recent advances in the fabrication, transfer, functional property, and application of freestanding oxide films are discussed in detail.

2 Preparation of freestanding oxide films

2.1 Mechanical exfoliation

Mechanical exfoliation is a technique that involves applying mechanical force to a 2D layered material, usually with tape, to separate single or multiple layers (or other thin deposited films) from the bulk material. This method provides a relatively straightforward approach for obtaining freestanding films. Since Novoselov et al.^[26] used the mechanical exfoliation method to obtain single-layer graphene from graphite in 2004, this method has received extensive attention. Researchers have continued to employ this method to prepare other 2D thin-film single-crystal materials, such as NbSe₂^[27] and Bi₂Te₃^[28]. Wang et al.^[29] successfully prepared BSCCO (Bi₂Sr₂CaCu₂O_{8+δ} and Bi₂Sr₂CaCu₃O_{8+δ}) single crystals with thicknesses of a few to a few tens of nanometers using mechanical exfoliation techniques. The temperature-dependent resistivity curve measured from the 30 nm thick sample exhibits superconductivity up to 87.2 K. The key to mechanical exfoliation is that the adjacent atoms in each layer of materials are bonded by covalent or ionic bonding with strong binding forces, while the layers are bonded together by van der Waals (vdW) forces with weak binding forces^[30,31], making it possible to strip single or few atomic layers from the bulk without damage.

In addition to directly obtaining freestanding films of one to several layers from the bulk of 2D layered materials, we can also deposit thin films onto 2D layered materials and then mechanically exfoliate them. This process engages vdW epitaxy. In contrast to conventional epitaxy, vdW epitaxy does not rely on one-to-one chemical bonds. Consequently, it is not restricted to materials with similar lattice structures. This liberates the epilayer to grow with its bulk lattice constant, despite a significant lattice mismatch that can reach 60%^[32,33].

Mica, a family of phyllosilicate minerals characterized by a monoclinic structure layered along the (001) plane, has recently been utilized as a substrate for the growth of functional oxides. Its ideal unit cell formula can be represented as X₂Y_nZ₈O₂₀(OH,F)₄, where X denotes interlayer cations (K⁺, Na⁺, Ca²⁺), Y denotes the octahedral coordinated elements (such as Al³⁺, Mg²⁺, Fe²⁺, Li⁺), and Z represents the tetrahedral coordinated elements (such as Si⁴⁺, Al³⁺)^[34], as depicted in Fig. 1a. Muscovite [KAl₂(Si₃Al)O₁₀(OH)₂; *a* = 5.17 Å, *b* = 8.94 Å, *c* = 20.01 Å, and β = 96°] is one of the most commonly used mica substrates for thin film fabrication processes. Fig. 1b shows the (001) basal plane of the cleaved muscovite mica surface with a hexagonally arrayed pattern of oxygen atoms. Fig. 1c shows the (100) projection of muscovite mica where the TOT (T: tetrahedral sheet; O: octahedral sheet) sandwich units are separated from each other by the vdW gap. These

sandwich units have very strong covalent bonding, while the sandwich units are weakly held together along the crystallographic *c*-axis. The key advantages of adopting a muscovite mica substrate include its 2D layered structures, atomically smooth surface, high thermal stability, chemical inertness, high transparency, mechanical flexibility, and compatibility with present fabrication methods^[34]. Many oxide materials have been prepared on muscovite, such as ZnO, SrTiO₃ (STO), MoO₂^[35], and CoFe₂O₄^[36] (Fig. 1d^[37]).

Directly using mica as a flexible substrate aside^[36–40], we are interested in mechanically exfoliating the upper target oxide film from mica substrates^[17,35,41]. Liu et al.^[17] deposited epitaxial SrRuO₃ (SRO) films on mica substrates with a BaTiO₃ (BTO) buffer layer, which was then mechanically exfoliated. The SRO/BTO film with 20 μm thick mica cleavage was separated from the bulk substrate by mechanical exfoliation using a sharp blade. The magnetic properties of the SRO films, including the Curie temperature, saturated magnetic moment, and coercive field, strongly depended on the mechanical strain. Flexible SRO films on mica substrates have been demonstrated to have highly tunable magnetic properties. Zhang et al.^[41] successfully deposited La_{0.7}Sr_{0.3}MnO₃ (LSMO) thin films on mica substrates using PLD techniques. The LSMO film was exfoliated off the substrate using 3 M tape, and the remaining mica fragments on the interface were removed using a blue protective film (NITTO SPV-KL-680) with less stickiness than the tape. Finally, a freestanding LSMO film was formed on the 3 M tape.

Like mica, graphene's structural characteristics and many advantages also make it suitable for many applications in mechanical exfoliation. For example, single-crystalline STO, BTO, CoFe₂O₄ (CFO), and Y₃Fe₅O₁₂ (YIG) were remote epitaxially (that is, by epitaxial growth of thin films seeded by the underlying substrate through a few layers of graphene) grown on graphene-coated STO, MgAl₂O₄ (MAO), and Gd₃Ga₅O₁₂ (GGG) substrates, respectively, by Kum et al.^[42]. They proposed this method as a universal mechanical exfoliation method to obtain freestanding oxide films. The utilization of the graphene buffer layer provides a weak vdW-bonded layer between the film and the substrate, preventing covalent bonding of the deposited film to the underlying substrate^[43]. Additionally, the 2D graphene layer is thin enough to allow the charge density of the substrate surface to penetrate, providing a surface potential for the deposited adatoms to align epitaxially with the underlying substrate^[44,44]. This demonstrates that the graphene-based remote epitaxy method enables covalently bonded materials to be easily mechanically exfoliated after deposition.

Heteroepitaxy on 2D layered materials provides a solution for exfoliating oxide membranes with high crystallinity and superior physical properties. In principle, no stress or strain is induced by the substrate across the contact plane, and the epilayer has a bulk ideal single-crystal-like crystalline quality. However, some issues still need to be paid more attention to. For example, it is still a challenge to generate an atomically flat surface of an epitaxially grown film. Moreover, for oxides with perovskite/spinel structures, only specific (111)-oriented films can be grown on a (001) mica substrate that exhibits a quasihexagonal arrangement of atoms on the surface.

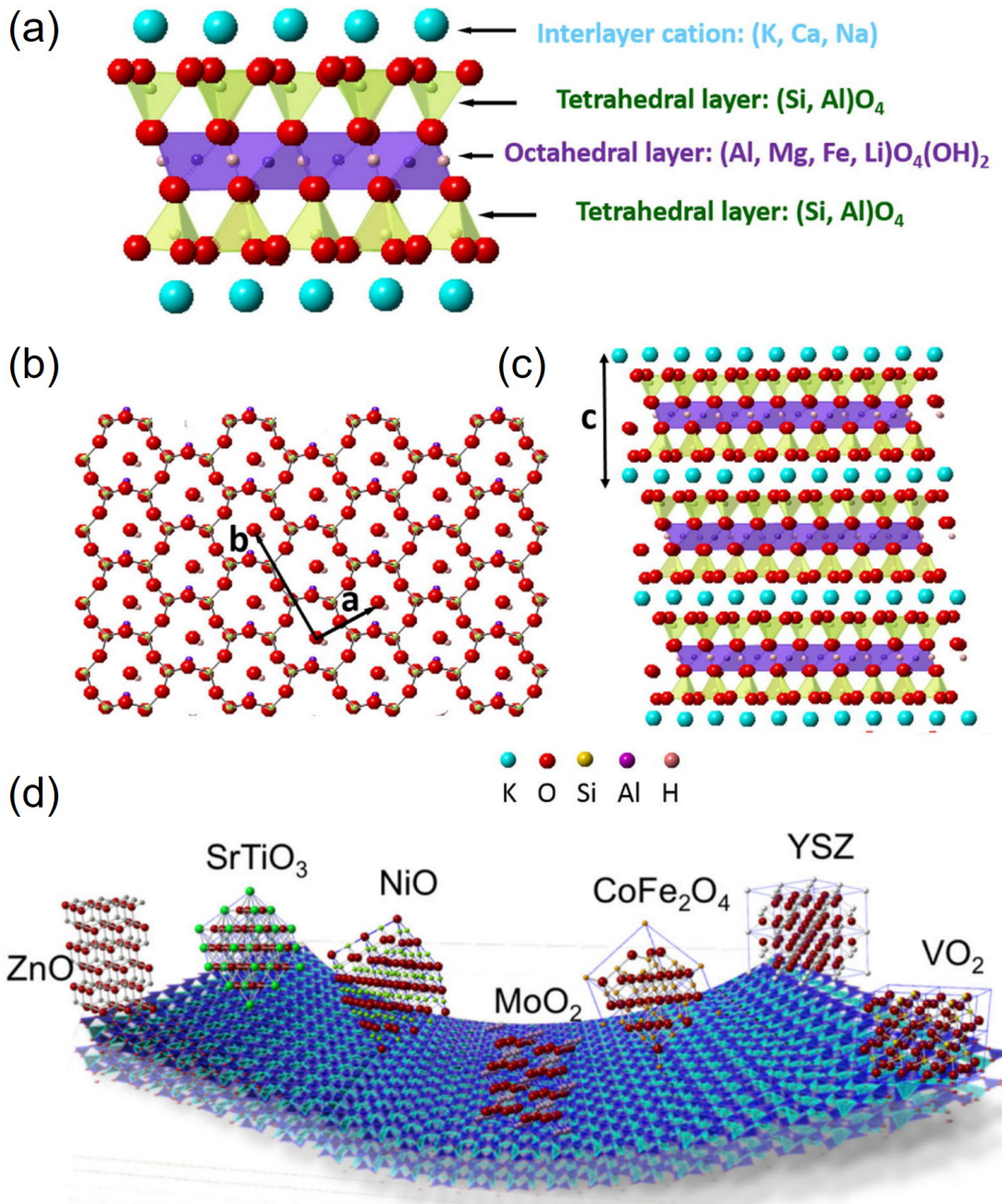


Fig. 1. (a) Structural unit of mica. Surface structure of muscovite mica: (b) (001) projection and (c) (100) projection. Reproduced with permission from Ref. [34]. Copyright 2017, Elsevier. (d) Summary of vdW oxide heteroepitaxy. Reproduced with permission from Ref. [37]. Copyright 2017, Springer Nature.

Because of the limited substrate orientation, a few reports exist on the integration of these materials with other structures, especially semiconductor devices.

2.2 Dry etching release methods

The dry etching release method refers to the use of plasma-activated chemical reactions or the bombardment of high-energy ion beams to remove substances. Here, the release of target film is achieved by selectively etching the interface

between the oxide film and the substrate. There are many types of dry etching release methods, including ion milling, reactive ion etching, electron cyclotron resonance plasma etching, induction coupled plasma etching, and laser lift-off (LLO) processes. Compared with other processes, the LLO process causes less damage to the film and is a more commonly used method. Point-by-point scanning of a point light source or line-by-line scanning after shaping the output beam of the laser into a line light source through optical compon-

ents allows the light to pass through the wafer or substrate, be incident on the junction of the film and the substrate, and evaporate the sacrificial layer with high absorption capacity by using the difference in the material's absorption of laser light, thereby realizing the separation of the substrate and the target film. The exfoliated films can be further transferred to other suitable substrates.

The LLO process was initially used to fabricate high-quality epitaxial GaN films for light-emitting diodes^[45,46] and has also been used for the preparation of oxide thin films. In 2000, Tsakalakos et al.^[47] successfully transferred (Pb, La) (Zr, Ti)O₃ films that were originally grown on (001) MgO substrates to stainless steel receptor substrates via the LLO process. During the LLO process, the ferroelectric properties of the film were well maintained. However, due to the bombardment of the laser, a damaged layer inevitably appears on the surface of the film. A brief ion-milling step involving immersion in an argon plasma with an accelerating voltage of 750 V was used to remove the damaged layer. In 2014, Jeong et al.^[48] reported their work on fabricating flexible Pb(Zr, Ti)O₃ (PZT) thin film-based energy harvesters using an LLO process. They used a XeCl pulsed excimer laser to transfer a PZT thin film from a sapphire wafer to a plastic substrate, and the piezoelectric properties of the transferred films did not degrade. In the work reported by Lee et al.^[49] in the same year, PZT was also transferred to a flexible substrate using an LLO process. Similar work was also mentioned in a 2017 article by Jeong et al.^[50], they prepared PZT films on double-sided polished MgO wafers and sapphire wafers. A 2D pulsed XeCl excimer laser was utilized to separate the PZT thin films from the rigid wafers. However, because of the limitations of sol-gel solution process, the prepared PZT thin films are polycrystalline.

While the LLO process is a simple and stable method that can achieve rapid and large-area stripping, it usually requires the selection of a substrate with a wide bandgap, such as sapphire, and laser energy positioned between the bandgap energy of the substrate and the film. However, this method inevitably causes damage to the interface, limiting its application.

2.3 Wet etching release methods

The wet etching release method is considered to be an effective approach for obtaining high-quality freestanding films^[22,51], generally causing less damage and better preserving the structural quality of the released membranes than physical release methods^[22]. This method involves growing a sacrificial layer (or buffer layer) on the substrate, then growing the desired film on this layer, and finally applying a suitable solution for selective etching to produce a freestanding film. However, the selection of both the sacrificial layer and the etchant is restricted by many parameters. For instance, the crystal structure and lattice constant of the sacrificial layer should align well with those of the substrate and the desired film. Furthermore, the sacrificial layer should be capable of being efficiently etched away without damaging the target oxide films.

As early as the 1980s, several freestanding films were prepared using this method^[52,53]. Detchprohm et al.^[52] grew a ZnO sacrificial layer on a sapphire substrate, followed by a GaN film, and then etched ZnO using aqua regia to obtain a freest-

anding GaN film. ZnO also acts as a buffer, making it easier to obtain GaN single crystals. In subsequent developments, much attention has been given to wet etching to prepare oxide films and heterostructures^[20,54–57]. For example, Bakaul et al.^[56] used PLD to grow single-crystal PZT on an LSMO-coated STO substrate. Then, the LSMO layer was wet etched in a diluted KI+HCl solution, releasing the layer(s) above it, which was then carried out by a transfer stamp based on polymethyl methacrylate (PMMA) and placed on a target substrate such as Si. The surface morphology and overall quality of the films remained almost unchanged before and after transfer. Shen et al.^[20] further improved upon Bakaul's work^[56] by preparing and transferring LiFe₅O₈ (LFO) thin films. They did not use PMMA in the transfer process but directly attached the destination substrate to the grown single-crystal LFO film. This improved method allowed them to successfully transfer larger, centimeter-sized (5 mm × 10 mm) single-crystal LFO films that still exhibited good magnetic properties.

In contrast to the previously mentioned techniques, Paskiewicz et al.^[54] did not prepare the sacrificial layer separately when using the wet etching technique to prepare the SRO nanomembrane but used the original STO growth substrate as the sacrificial release layer. They first patterned the nanomembrane area and then used selective chemical etchants to etch the interface regions between the film and the substrate to remove the underlying material, thereby releasing the nanomembrane materials from the original substrate. Selective removal of the substrate after growth is a direct approach for obtaining freestanding epitaxial oxide films^[58–60], but because of the high cost and time consumption due to the large volume needed for etching, this method is usually replaced by other methods.

A major advance in wet etching technology is the use of water-soluble sacrificial layers such as Sr₃Al₂O₆ (SAO) to prepare freestanding oxide films^[22]. Compared with etching with chemical solutions (acidic solutions), etching with water will greatly reduce contaminants caused by etchant solutions.

As shown in Fig. 2, SAO forms a cubic unit cell (space group Pa3) with a lattice constant of $a=15.844$ Å, which closely matches the four unit cells of the most representative perovskite substrate, STO, as is clear from the two structures projected onto the (001)-plane (Fig. 2c^[22,61]). This close resemblance in the lattice forms the strong basis for the epitaxial growth of the SAO sacrificial layer on the STO substrate. A key aspect of the Al–O network in SAO is that it consists of discrete 12-membered (Al₆O₁₈)¹⁸⁻ rings that easily hydrolyze in water (Fig. 2b), which lays the foundation for the smooth hydrolysis of the sacrificial layer and leaves no contaminants. In addition, the SAO surface preserves the perovskite step-and-terrace structures of the underlying STO substrate, and its thickness can be controlled during growth, which allows the surface of the SAO thin film to act as a template for subsequent atomic-scale perovskite growth.

Lu et al.^[22] grew various perovskite films, including STO, LSMO, and their superlattices (SLs), on a SAO buffer layer, followed by exfoliation and transfer, as shown in Fig. 2a. Their work demonstrated the versatility and superiority of this method using SAO as an epitaxial sacrificial layer to

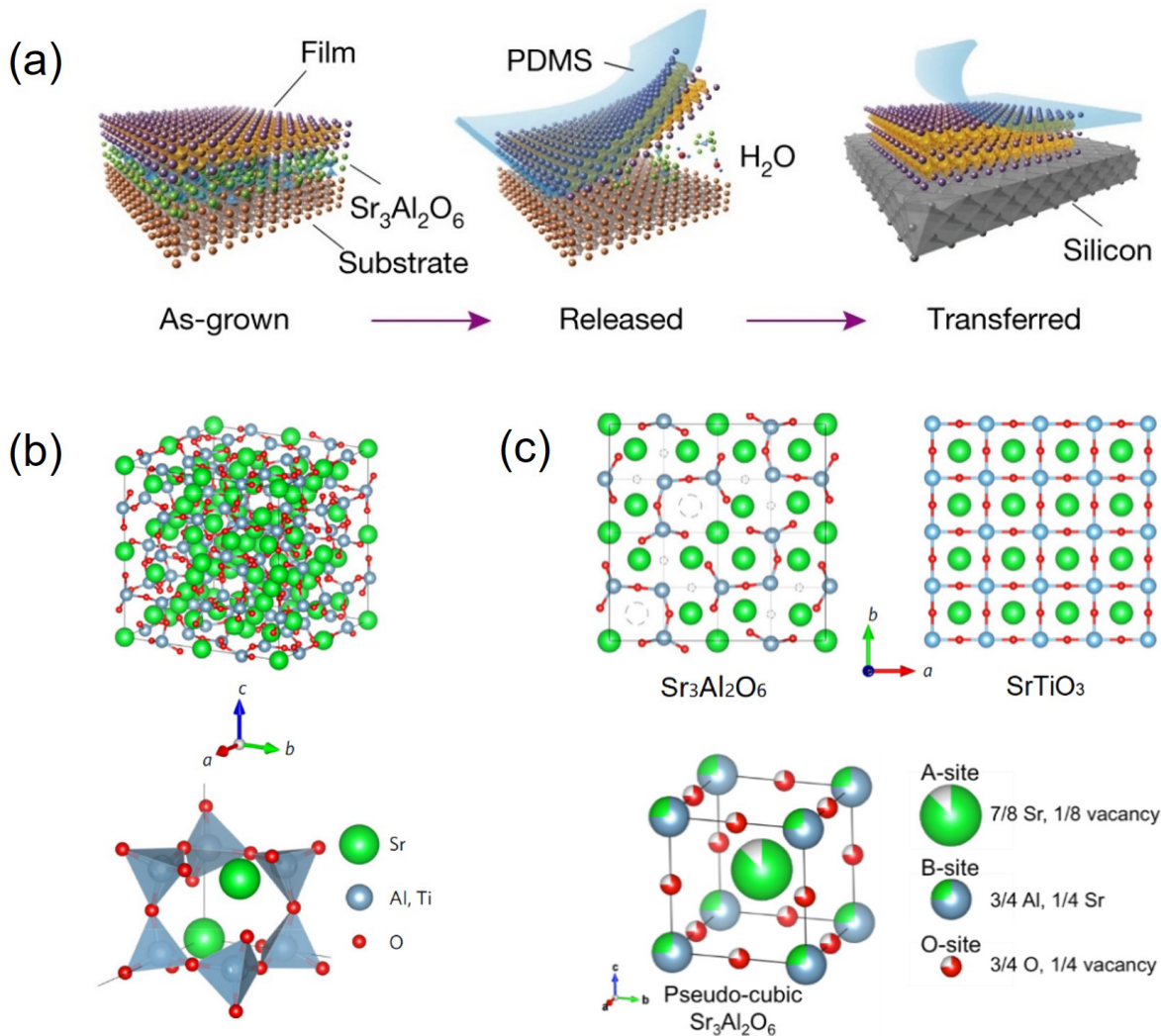


Fig. 2. (a) Process schematic for oxide membrane release and transfer. Reproduced with permission from Ref. [71]. Copyright 2019, Springer Nature. (b) Cubic lattice structure of SAO and Al_6O_{18} rings consisting of AlO_4 tetrahedra. Reproduced with permission from Ref. [22]. Copyright 2016, Springer Nature. (c) (Top) Top 1/4 of the SAO unit cell projected onto the (001) plane, dashed circles indicate vacancy sites, and 4x4 unit cells of the STO crystal structure projected onto the (001) plane. Reproduced with permission from Ref. [22]. Copyright 2016, Springer Nature. (Bottom) Schematic illustrating the pseudocubic unit cell of SAO. Reproduced with permission from Ref. [61]. Copyright 2017, American Institute of Physics.

fabricate perovskite oxide thin films, which was widely used in subsequent studies^[62–69]. Hong et al.^[70] grew STO films with different thicknesses on the SAO sacrificial layer and studied the structural evolution of STO in the 2D limit. All STO films were initially single-crystalline before release from the bulk substrate, but for freestanding STO films after release, the films changed from single-crystalline to amorphous (with a critical thickness of 5 u.c.) as they became thinner. However, their work was overturned by Ji et al.^[71] in 2019. In Ji’s work, epitaxial SAO and subsequent perovskite oxide thin films were grown by reactive molecular beam epitaxy with carefully optimized growth conditions. The final prepared freestanding STO films were characterized by TEM using selected-area electron diffraction (SAED) and plane-view and cross-sectional high-angle annular dark-field (HAADF) imaging with atomic resolution. They demonstrated that it is possible to synthesize freestanding perovskite oxide films down to a thickness of 1 u.c. (well below 5 u.c.) and transfer them with high crystalline quality.

The SAO sacrificial layer has been largely used for growing perovskite oxides due to its facile dissolution in water and good structural and chemical compatibility with perovskite oxides, but its lattice constant may not be suitable for all target oxide films. To address this issue and improve the film quality, the solid-solution family of $(\text{Ba,Sr,Ca})_3\text{Al}_2\text{O}_6$ is proposed, which can achieve continuous tuning of the sacrificial layer lattice constant from 0.382 nm (Ca 100%) to 0.413 nm (Ba 100%), covering the lattice constant range of the vast majority of perovskites and related oxides. Singh et al.^[72] prepared high-mobility transparent conducting oxide La-doped BaSnO_3 freestanding films using SAO and $\text{Ba}_3\text{Al}_2\text{O}_6$ water-soluble sacrificial layers. The 4 at. % La-doped BaSnO_3 ($\text{La}:\text{BaSnO}_3$) prepared in their work has a lattice mismatch of 4% with SAO and 0.21% with $\text{Ba}_3\text{Al}_2\text{O}_6$. When SAO was used as the sacrificial layer, the released film had a high crack density, while with the epitaxial $\text{Ba}_3\text{Al}_2\text{O}_6$ sacrificial layer, crack-free $\text{La}:\text{BaSnO}_3$ membranes on the millimeter scale were prepared. Minimizing the lattice mismatch is a critical

factor in preventing crack formation in release membranes. Another example is the preparation of STO thin films by Xu et al.^[73] using $\text{Sr}_2\text{CaAl}_2\text{O}_6$ as a sacrificial layer, with a lattice constant of 15.6 Å, which is nearly four times that of STO. The use of the $\text{Sr}_2\text{CaAl}_2\text{O}_6$ sacrificial layer effectively reduced the lattice mismatch between different layers and cracks in the prepared film.

Recently, a complementary sacrificial layer to the widely used $\text{Sr}_3\text{Al}_2\text{O}_6$, super-tetragonal $\text{Sr}_4\text{Al}_2\text{O}_7$ (SAO_T), was reported by Zhang et al.^[74] The biaxial-strained SAO_T film has a tetragonal structural symmetry. Such a low-symmetry crystal structure of SAO_T enables superior flexibility under epitaxial strain and thus wide-range tunability of in-plane lattice constants. The resultant coherent growth of high-quality $\text{ABO}_3/\text{SAO}_T$ epitaxial heterostructures considerably improves the crystallinity and integrity of water-released freestanding oxide membranes. For a variety of nonferroelectric oxide membranes (3.85 Å to 4.04 Å), the crack-free areas can span up to a millimeter in scale. The corresponding functionalities are comparable to the epitaxial counterparts. The SAO_T sacrificial layer offers a versatile and feasible experimental approach to producing large-scale, crack-free freestanding oxide membranes.

To date, several high-quality single-crystalline oxide films or multilayers have been successfully made freestanding by utilizing water-soluble layers as sacrificial layers. Although promising, the high reactivity of water-soluble sacrificial layers also leads to difficulty in synthesis and poor stability in ambient air. Although Li et al.^[75] proposed a strategy to stabilize the SAO sacrificial buffer layer by utilizing an ultrathin capping layer of STO, it remains to be seen whether this technique can be universally applied.

2.4 Transfer methods

While most current works are focused on different etching methods, the upper limit of the film area and quality is usually dependent on the lift-off and transfer steps. The key issue for good transfer is preventing crack formation and minimizing contamination. Current oxide film transfer methods typically use well-developed transfer methods designed for graphene transfer^[76]. A conventional method involves the use of organic support materials for easy handling. A support layer, e.g., polyimide (PI) tape^[20], polydimethylsiloxane (PDMS), polymethylmethacrylate (PMMA)^[56] or polystyrene (PS), is employed and coated on the whole film surface before the etching process to prevent fracture. Then, the sacrificial layer is selectively etched, the oxide film is transferred to other target substrates, and the support layer is finally removed by mechanical detachment, thermal decomposition, or acetone. The use of a polymeric support layer, while facilitating transfer, also acts to prevent crinkling or folding of the freestanding film during the etching and transferring process.

Fig. 3 shows four transfer methods based on the wet etching approach that have been studied for transferring oxide thin films. In method I, PMMA is used as the support layer, which can eventually be rinsed off with acetone. This method is commonly used in the transfer of graphene but is not applicable for oxide thin films because the films have high densities compared to graphene, which makes it difficult for the

films to float on the surface and detach from the substrate. In 2016, Bakaul et al.^[56] proposed an improved method for transferring single-crystal ferroelectric thin films onto silicon and other substrates using PMMA as a handle, with integrated film thicknesses very small, down to a single unit cell. However, the size of the single-crystal film transferred by this method is small, and it is easy to introduce contamination during the transfer process, which makes the subsequent use of the film inconvenient. In method II, the target film is directly attached to the PI tape. This method has been shown to transfer large-area oxide films^[20, 77], but it is almost impossible to release the films to other substrates, and the resulting freestanding film must adhere to PI tape. The support layer used in method III is a thermal release tape (such as PDMS), which can be removed by heating rather than using chemicals. However, due to factors such as stress caused by heating, the appearance of voids, cracks, and some residues from the thermal release tape is inevitable after the transfer, making it difficult to obtain a continuous film.

Method IV is a new method proposed by Zhang et al.^[68], which is an improvement on method I. Different from the previous methods, this method uses a two-layer structure support layer. A PMMA solution was spin-coated onto the surface of the target film and allowed to dry before attaching the tailored PET film. The additional PET frame on PMMA prevents the film from sinking, overcoming the shortcomings of method I. In addition, the PET membrane is much more mechanically stable than the PMMA layer, allowing the freestanding film to be carefully manipulated without flexing, which reduces film cracking. The use of two-layer structural support layers is not uncommon. For example, Chen et al.^[78] used a PET/silicone support layer to transfer large-area high-quality graphene, Lu et al.^[22] used PET/silicone to transfer various perovskite films, and later used a PPC/PDMS support layer to transfer the grown BTO/LSMO/BTO ferroelectric tunnel junction (FTJ)^[62]. The combined use of different polymer materials can compensate for the shortcomings of each material and expand the selection range of the support layer, providing more possibilities for the transfer of freestanding films.

3 Strain engineering in freestanding oxide films

The profound interplay between structural and electronic properties is one of the most interesting strategies to control functionalities in perovskite oxides, and epitaxial oxide films are largely influenced by strain^[79, 80]. Traditional thin films are strictly bound to substrates, a limitation that hinders their changes in stress and further applications, but it is anticipated that more unusual properties will emerge when single-crystalline functional oxide thin films are fabricated into 2D structural forms^[81]. Freestanding thin films are emerging as a new platform for investigating extremely large and tunable strain states in oxides. Oxide films can be mechanically coupled to an external platform without an epitaxial relationship, for which strain states of different symmetries can be freely chosen by design^[21, 23]. The common strategies for controlling strain in membranes are mechanical stretching and

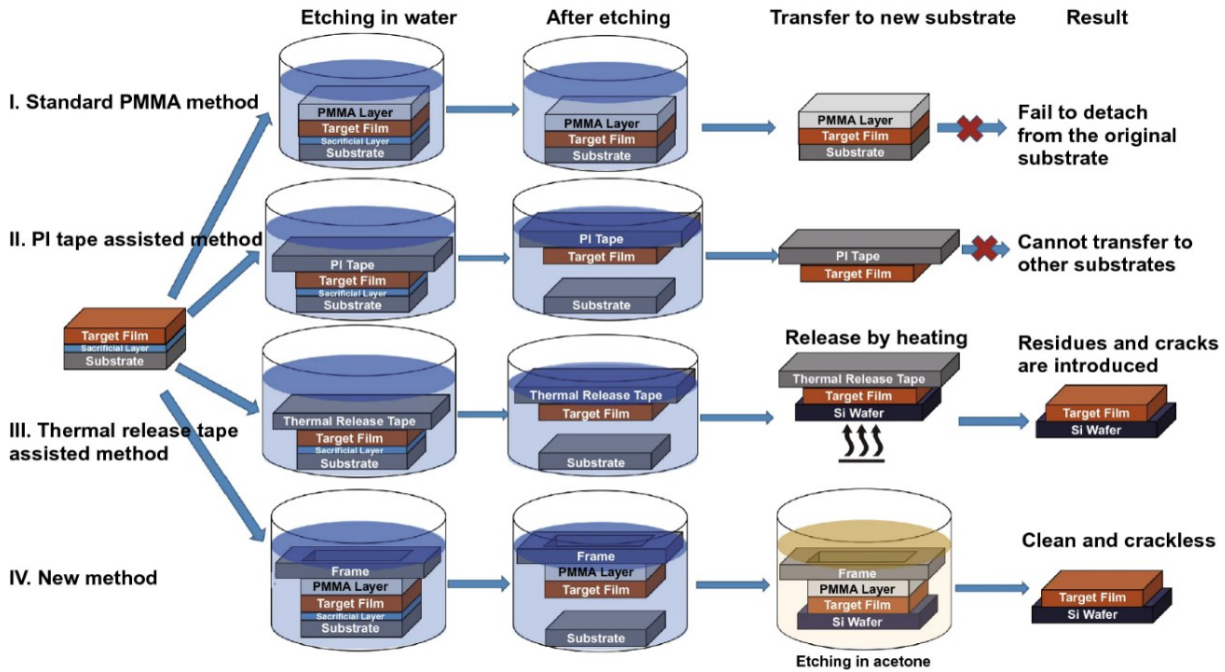


Fig. 3. Schematics of four different wet-etching-based methods for fabricating oxide films. Reproduced with permission from Ref. [68]. Copyright 2021, Springer Nature.

mechanical bending.

3.1 Mechanical stretching

Strain engineering in perovskite oxides provides dramatic control over the material structure, phase, and properties but is restricted by the discrete strain states produced by commercially available single-crystal substrates. The development of freestanding complex oxide membranes both circumvents the challenges of difficult application of large strain through epitaxial strain and provides unique opportunities to realize previously unobserved strain-induced responses.

Using the epitaxial lift-off strategy to release oxide membranes and transfer them to stretchable polymer substrates, Hong et al.^[23] controlled the strain state of freestanding $\text{La}_{0.7}\text{Ca}_{0.3}\text{MnO}_3$ membranes by external forces. As shown in Fig. 4, they leveraged access to these extreme strain states to both modulate the transport properties of $\text{La}_{0.7}\text{Ca}_{0.3}\text{MnO}_3$ and stabilize a nonequilibrium phase of the $\text{La}_{0.7}\text{Ca}_{0.3}\text{MnO}_3$ membranes under different biaxial strains from 1% to 5% and different uniaxial strains from 1% to 8%. Uniaxial and biaxial strains suppressed the ferromagnetic metal at distinctly different strain values, inducing an insulator that can be extinguished by a magnetic field. Following this approach, the physical properties of the $\text{La}_{0.7}\text{Ca}_{0.3}\text{MnO}_3$ film were characterized under various magnetic fields, temperatures, and strain states to construct a phase diagram as a function of the biaxial strain and magnetic field (Fig. 4b, d).

The interest in this straining method later shifted to the control of polar order. Xu et al.^[74] integrated freestanding STO films onto a flexible polymer stretching platform to probe the strain-tunable ferroelectric transition in STO. They characterized the ferroelectric properties of strained STO via PFM at room temperature. In a small strain state ($\epsilon \leq 1.25\%$), very weak signals from the membrane were observed, indicating the absence of ferroelectricity at room temperature within this

strain range. In contrast, for larger strains ($\epsilon > 1.5\%$), strong lateral signals from membranes with notable stripe domain patterns indicated the emergence of room-temperature ferroelectricity.

3.2 Mechanical bending

Strain control can also be achieved via mechanical bending,

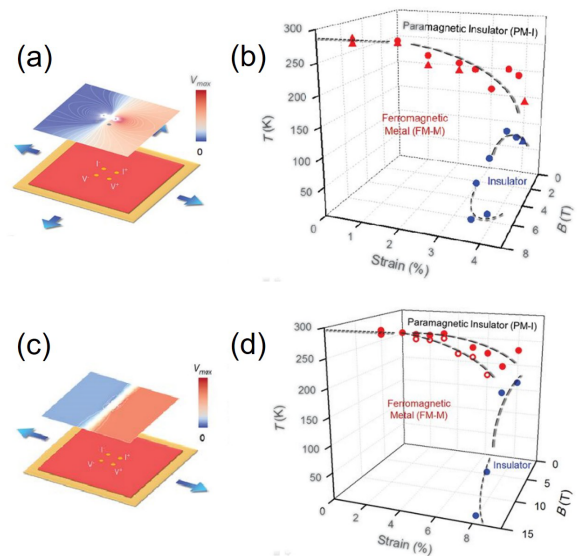


Fig. 4. Phase diagram of biaxially strained and uniaxially strained $\text{La}_{0.7}\text{Ca}_{0.3}\text{MnO}_3$ membranes. (a) Electric potential mapping of the central van der Pauw (vdP) geometry in membranes. (b) Phase diagram of biaxially strained LCMO membranes. (c) Electric potential mapping of the central vdP geometry in membranes under uniaxial strain with 1:100 resistivity anisotropy. (d) Phase diagram of uniaxially strained LCMO membranes. Reproduced with permission from Ref. [23]. Copyright 2020, American Association for the Advancement of Science.

which is different from simple stretching and affects the polarization and other properties of films. Hwang's group^[82]

presented nanomechanical measurements of freely suspended STO crystalline membrane drumheads (Fig. 5a). An unexpect-

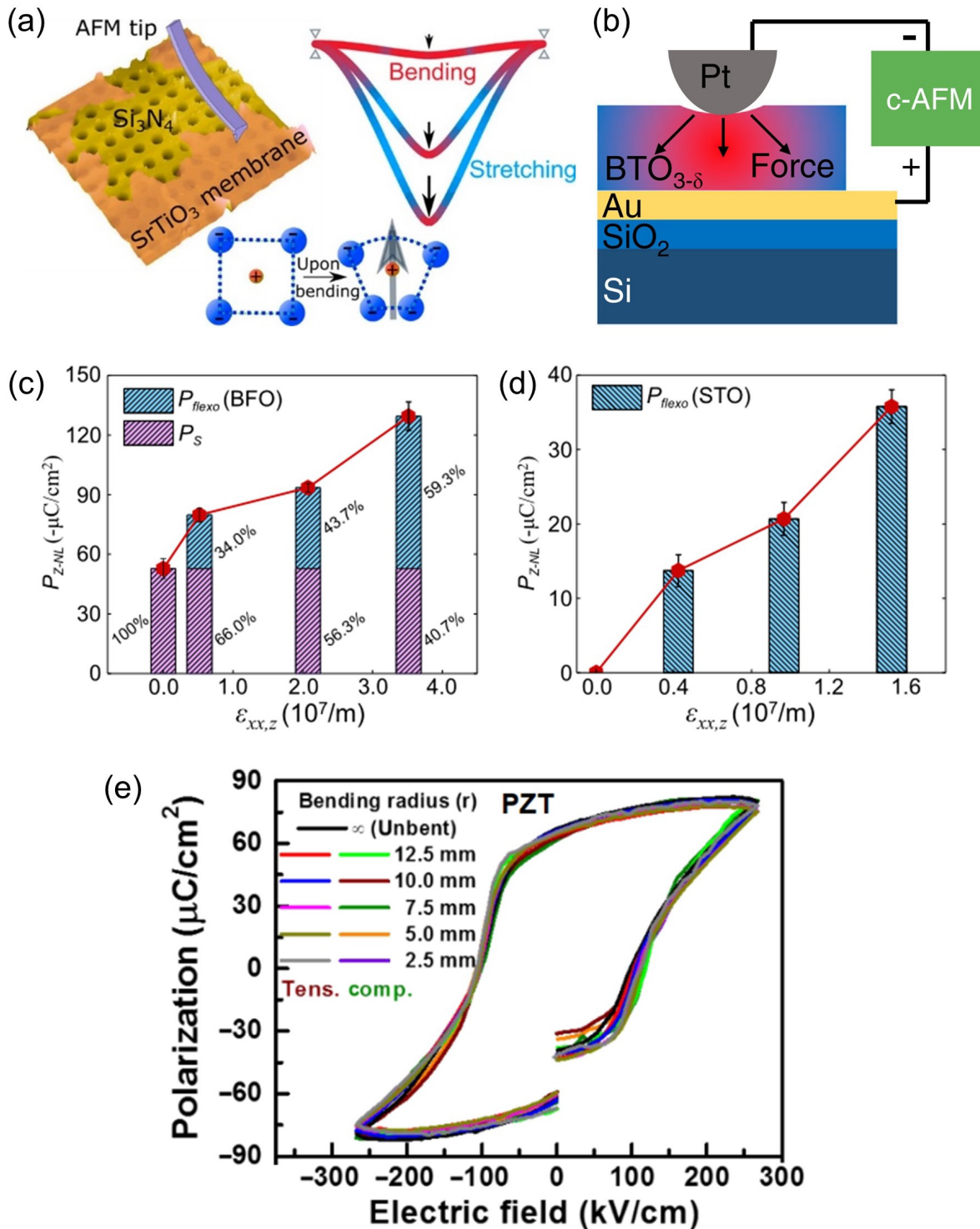


Fig. 5. (a) Schematic of strain gradient elasticity in freely suspended STO crystalline membrane drumheads. Reproduced with permission from Ref. [82]. Copyright 2021, American Chemical Society. (b) Illustration of the experimental configuration of the conductive AFM (c-AFM) test, which was used to examine the flexoelectricity of the transferred $\text{BTO}_{3-\delta}$ films. Reproduced with permission from Ref. [84]. Copyright 2022, Springer Nature. (c, d) The out-of-plane polarizations at the neutral layer (where the in-plane strain is near zero) P_{Z-NL} and their corresponding strain gradients $\epsilon_{xx,z}$ from the bent BFO and STO membranes, respectively, where P_s is spontaneous polarization. The error bars represent the standard deviation of the measured unit cells. Reproduced with permission from Ref. [86]. Copyright 2022, Springer Nature. (e) Polarization-electric field (P-E) hysteresis loops under various tensile and compressive bending radii. Reproduced with permission from Ref. [18]. Copyright 2017, American Association for the Advancement of Science.

ted nonmonotonic thickness dependence of the Young's modulus upon small deflections was observed. In addition, the modulus inferred from the predominant bending deformation was three times greater than that inferred from the predominant stretching deformation for membranes thinner than 20 nm. These results visibly demonstrated that nanoscale STO exhibited sharply different bending and stretching rigidities, raising the possibility for new dynamics in nanoelectromechanical devices^[82,83]. Da et al.^[84] used an AFM tip to apply different loading forces on a freestanding $\text{BTO}_{3-\delta}$ (oxygen-deficient BTO) film and studied the changes in the strain gradient and polarization (Fig. 5b). The $\text{BTO}_{3-\delta}$ films possessed enhanced flexoelectric properties with a gauge factor as high as 1127.

In addition, Guo et al.^[85] demonstrated the continuous tunability of the photoconductance by bending a freestanding BiFeO_3 (BFO) film. The bending-induced controllable strain gradient generated an additional electric field by the flexoelectric effect, which coupled with the BFO polarization-dependent internal electric field, finally leading to tunable photoconductance in freestanding BFO. The strategy they proposed provided an alternative way to tailor the physical properties of flexible devices. Similarly, Cai et al.^[86] observed significant polarization enhancements by bending freestanding BFO and STO films, revealing that flexoelectricity plays an important role in determining polarization (Fig. 5c,d).

Functional oxides can also be directly grown on flexible substrates to obtain bent states by bending the original substrates, which is a supplement to the freestanding strategy. For example, single-crystalline flexible ferroelectric zirconium titanate (PZT) fabricated directly on a flexible mica substrate via vdW epitaxy exhibits remarkable mechanical properties with robust operation in bent states. Fig. 5e shows that under the bent state with a bending radius from 12.5 mm to 2.5 mm, no obvious changes are observed in the polarization-electric field (P-E) hysteresis loops for either tensile or compressive strain^[18]. Huang et al.^[87] demonstrated the growth of $\text{La}_{0.67}\text{Sr}_{0.33}\text{MnO}_3$ thin films on mica substrates and their functionalities. The films presented excellent mechanical stretchability and property stability under mechanical bending conditions. Furthermore, a study has shown that the magnetic properties of flexible SRO/BTO/mica films can be highly tuned by applying controllable mechanical strain, showing great potential for novel applications in flexible electronics^[17].

4 Emerging functionalities in freestanding oxide films

Generally, the ionic or covalent bonds in oxides have great interaction strength and lack sufficient slip systems for dislocation movement under deformation, leading to brittle fracture. However, it can be different for freestanding oxide films. The freestanding BTO membranes were found to undergo $\sim 180^\circ$ folding during an in situ bending test, demonstrating superelasticity and ultraflexibility^[88] (Fig. 6a). The superelasticity was thought to originate from the dynamic evolution of ferroelectric nanodomains. High stresses markedly modulate the energy landscape and allow dipoles to rotate continuously between the *a* and *c* nanodomains. A continuous transition

zone is formed to accommodate the variant strain and avoid the high mismatch stress that usually causes the formation of fractures^[88]. Researchers have also predicted that this phenomenon could occur in other ferroelectric systems through domain engineering. As expected, the freestanding single-crystalline BFO films exhibit superior flexibility, with a maximum bending strain of up to 5.42% during in situ bending under scanning electron microscopy. This superior elasticity mainly originates from the reversible rhombohedral-tetragonal phase transition, as revealed by phase-field simulations^[89]. Additionally, many freestanding films, including BiMnO_3 ^[90] and Fe_3O_4 ^[91], have also demonstrated superflexibility.

In self-assembled membranes, periodic wrinkles are usually designed and fabricated to provide distinct functionalities. Because of their excellent flexibility, freestanding BTO films were further fabricated into wrinkle patterns with finely controlled parallel, zigzag, and mosaic patterns. The wrinkled BTO films show periodically alternating peak and valley morphologies. The IP and OOP PFM measurements also demonstrate the corresponding periodic variations in the amplitude and phase (Fig. 6b–d). The valley region (compressive strain/strain gradient) shows the strongest mean piezoresponse in the OOP direction, and the peak region (tensile strain/strain gradient) shows the strongest mean piezoresponse in the IP direction. The polarizations of the domains in the valley regions mainly point along the OOP direction, while those in the peak regions primarily point along the IP direction. The excellent elasticity and the correlated coupling between the polarization and strain/domain gradient are strongly associated with ferroelectric domain switching and continuous dipole rotation. The out-of-plane polarization is primarily generated in compressive regions, while the in-plane polarization dominates in tensile regions. Additionally, an enhanced piezoelectric response and significant flexoelectricity are also observed in these wrinkled BTO membranes^[24].

Nevertheless, the piezoelectric properties of freestanding membranes have remained elusive. Elangovan et al.^[92] showed that under external electric fields, freestanding BTO membranes underwent controllable and reversible “sushi-rolling-like” 180° folding-unfolding cycles (Fig. 6e, f). Giant $>3.8 \mu\text{m}$ and $4.6 \mu\text{m}$ displacements for a 30 nm thick membrane were observed at room temperature and 60°C , respectively, and further increasing the electric field above the coercive value was found to change the fold curvature, thereby augmenting the effective piezoresponse.

In addition, novel lateral twisting/boundary states and high-density switchable polar skyrmions have also received much attention from researchers. By transferring a freestanding film with different crystalline orientations onto the substrate before growing the film, the twist angle can be adjusted, and a twisted oxide lateral homostructure with controllable in-plane conjunctions can be obtained. This novel structure results in new phenomena and new properties. Using this method, Wu et al.^[93] reported enhanced second harmonic generation and exotic magnetotransporter behaviors, and Chen et al.^[94] reported the creation of morphotropic grain boundaries in laterally interconnected cobaltite homostructures. In freestanding PTO/STO bilayers transferred onto silicon, Han et al.^[95] observed high-density (approximately 200 Gbit per square

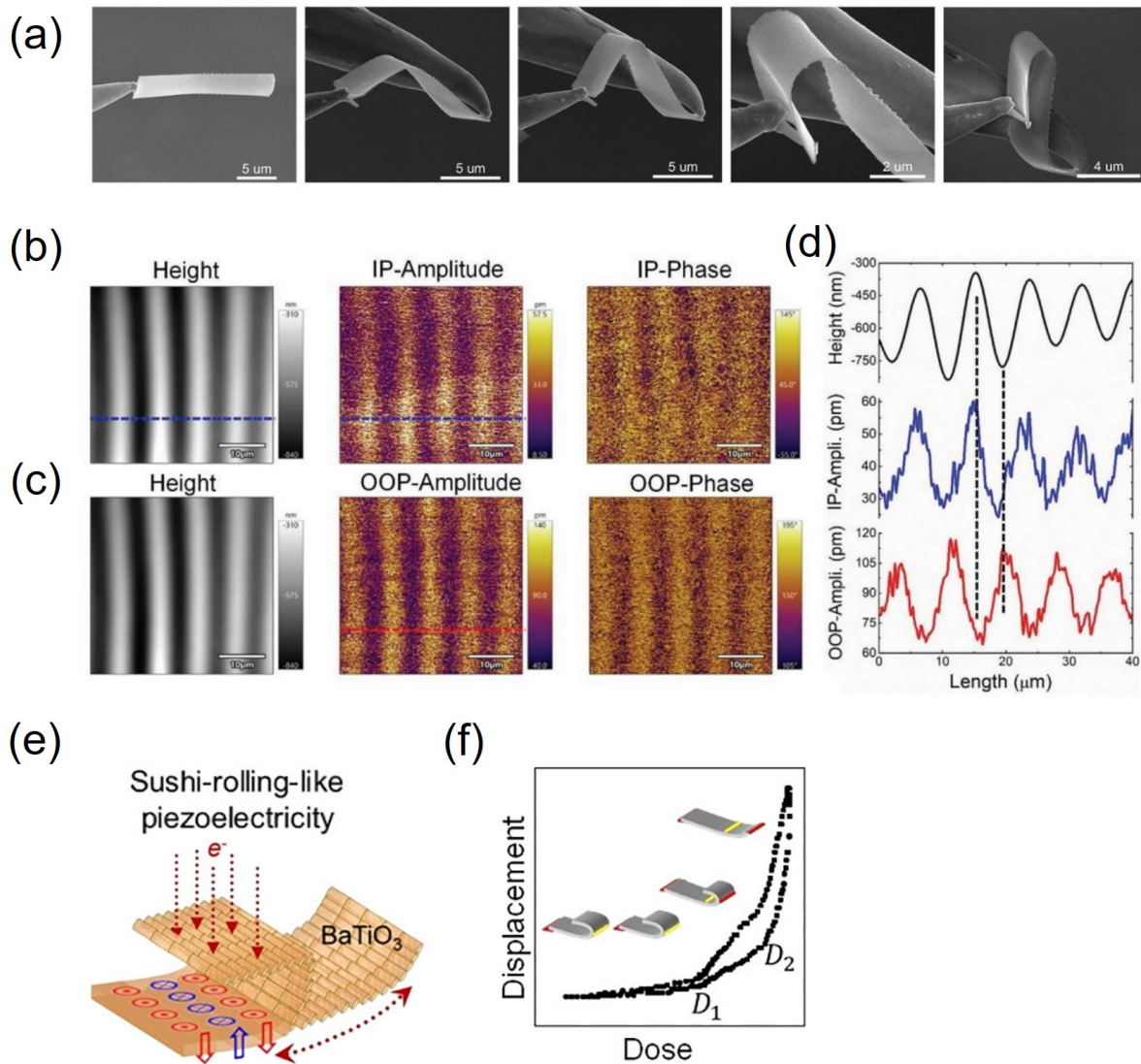


Fig. 6. (a) Series of SEM images of the bending process of a BTO nanobelt ($20\ \mu\text{m} \times 4\ \mu\text{m} \times 120\ \text{nm}$). Reproduced with permission from Ref. [88]. Copyright 2019, American Association for the Advancement of Science. (b, c) PFM images and measurements of wrinkled BTO films. (b) IP-PFM images. (c) OOP-PFM images. (d) Line profiles of the corresponding height and amplitude data (average of 20 pixels) along the blue dotted lines in (b) and (c). Reproduced with permission from Ref. [24]. Copyright 2020, John Wiley and Sons. (e, f) Electromechanical cycles in BTO. (e) Schematic illustration of the membrane's electromechanical structure. (f) Displacement of the membrane fold front versus dose (equivalent to the electric field) for cycling results in a reversible and reproducible electromechanical response. Reproduced with permission from Ref. [92]. Copyright 2020, American Chemical Society.

inch) skyrmion-like polar nanodomains, which could be converted between two types (center divergent and center convergent) by applying an external electric field (PTO, lead titanate), providing a way to design nonvolatile memories.

Depending on whether 2D films are used as freestanding monolayers or are stacked into bilayers or multilayers, a wide variety of property phenomena arise, which can deviate significantly from the behavior of the bulk crystal, leading to a variety of novel properties. The successful fabrication and transfer of one-unit-cell-thick ultrathin single-crystalline freestanding STO films have been demonstrated by Ji et al.^[71] In addition, by synthesizing BFO ultrathin films based on water-soluble SAO as the sacrificial buffer layer and transferring them to diverse substrates, they found that freestanding BFO films exhibit unexpected and giant

tetragonality and polarization when approaching the 2D limit (Fig. 7a). An R-like to T-like phase transition can be observed in Fig. 7b as the freestanding BFO film approaches the 2D limit. In bulk rhombohedral BFO, the stereochemical activity of a lone pair of Bi electrons drives off-centering; in a T-like phase, Fe also displaces from the centrosymmetric position, the combined effects of which result in a large c/a ratio. In ultrathin films, the surface electric field further displaces the polar surfaces and enhances the c/a ratio. By releasing the clamping imposed by the substrate in BFO freestanding films, the in-plane lattice constants decrease, and the out-of-plane lattice constants further increase, resulting in a very large c/a value of 1.22.

The dominant effect of substrate clamping can also limit the electromechanical response and often leaves electrostat-

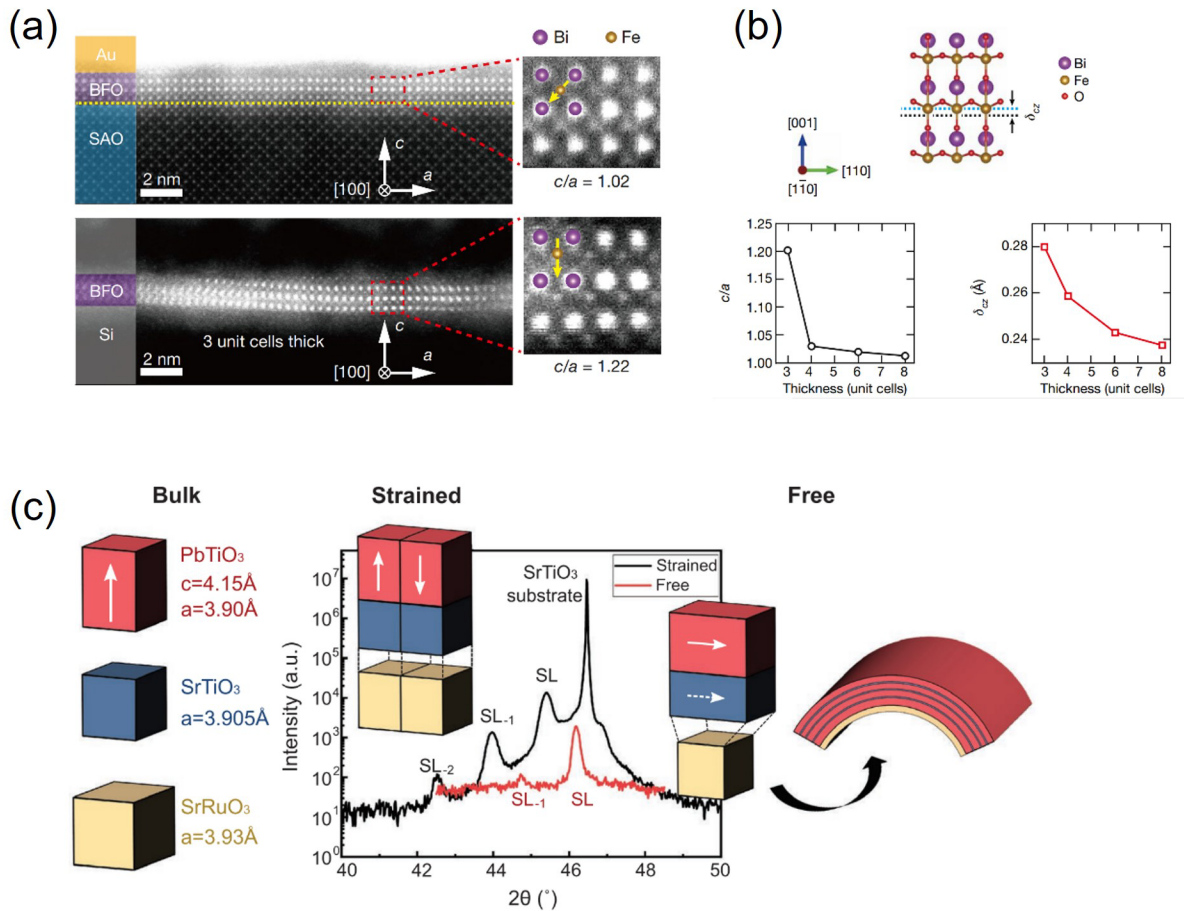


Fig. 7. (a) Cross-sectional HAADF images of a three-unit-cell BFO film before (top) and after (bottom) releasing the film, showing an R-like phase with polarization along the $\langle 111 \rangle$ direction and a T-like phase with polarization along the $\langle 001 \rangle$ direction, respectively. (b) Calculated giant polarization and lattice distortion in ultrathin freestanding BFO films. The off-center displacement ($\delta_{z,z}$) is defined as the distance along the out-of-plane direction between the centers of the neighboring Bi ions (dotted black line) and Fe ions (dotted blue line). Reproduced with permission from Ref. [71]. Copyright 2019, Springer Nature. (c) XRD $\theta-2\theta$ scans for the strained and freestanding superlattice films. Schematics showing the relationship between the lattice parameters for the bulk materials (left), the favored polarization configuration for the strained heterostructure (middle inset), and the mismatch between the in-plane lattice parameters of the freestanding superlattice and the bulk lattice parameter of the SRO electrode, which causes the heterostructure to bend (right). Reproduced with permission from Ref. [96]. Copyright 2022, John Wiley and Sons.

ics to play a secondary role, but releasing epitaxial multilayers from their underlying substrates can overcome these restrictions and harness the full potential of strain and electrostatic engineering. Li et al.^[96] investigated freestanding superlattices of PbTiO_3 and STO with an SRO bottom electrode. When it was released from its substrate, an electrostatically driven transition from a predominantly out-of-plane polarized to an in-plane polarized state was observed. In turn, the appearance of an in-plane polarization created a large mismatch between the lattice constants of the superlattice and the bottom SRO electrode, causing the whole structure to curl into microtubes with a well-defined radius of curvature. Fig. 7c shows the $\theta-2\theta$ scans around the 002pc reflection for the (14|3) superlattice before and after release. Upon release, because of the bending of the rolled-up freestanding film fragments, which rotate most of the film volume out of the Bragg condition, the overall intensity of the diffraction signal is greatly reduced. The presence of a faint SL-superlattice satellite demonstrated that the superlattice structure remained intact.

Overall, many novel phenomena of freestanding oxide films appear at the nanoscale. These phenomena and the corresponding microstructural arrangements have attracted much interest from researchers. In particular, there have been many studies on the 2D limitations of freestanding films. These novel phenomena and unique properties demonstrate significant potential for further new discoveries in freestanding oxides, bringing us both interesting and challenging research subjects.

5 Functional devices

The well-preserved physical properties of freestanding functional oxide films provide a broad platform for designing nanodevices with complex functions. Freestanding films of oxide single crystals and heterostructures can be combined with semiconductor device architectures, flexible electronics, and a growing family of exfoliated 2D materials^[97-99], as they can be directly compatible with established device designs and processing approaches used in semiconductors.

Integrating freestanding oxide films with 2D semiconductors or silicon to make transistors solves many of the difficulties of traditional methods, such as growing high-quality dielectrics on 2D materials without dangling bonds and direct epitaxial synthesis of functional complex oxides on Yang et al.^[100] prepared STO thin films on SAO sacrificial layers, exfoliated them, and transferred them onto molybdenum disulfide (MoS_2) to finally fabricate field effect transistors (FETs). Fig. 8a shows the variation in the source-drain current (I_{DS}) with the top-gate voltage (V_{TG}) in MoS_2 transistors with STO top-gate dielectrics (the optical image is shown in the inset of Fig. 8a) when the source-drain bias voltage (V_{DS}) is 0.5 V and 50 mV and the back gate is grounded. The MoS_2 transistors exhibit an on/off current ratio of 10^8 at a V_{DS} of 0.5 V and a subthreshold swing value as small as $66 \text{ mV}\cdot\text{dec}^{-1}$, close to the thermionic limit at room temperature ($60 \text{ mV}\cdot\text{dec}^{-1}$). Fig. 8b shows the variation in I_{DS} with V_{DS} . The output curves are linear when V_{DS} is small, indicating ohmic contacts. When V_{DS} further increases, I_{DS} gradually saturates, signaling pinch-off of the MoS_2 channel at a larger V_{DS} . In addition, PZT was also transferred onto the surface of Si/SiO₂ and used as the gate of a silicon-on-insulator (SOI) transistor^[56], which shows clear control of the channel charge with ferroelectric polarization, as evidenced by the signature anti-clockwise hysteresis loop and an abrupt jump in the current.

In recent years, advancements in the preparation techniques of ferroelectric films have led to increased attention given to FTJs. Freestanding technology also provides a way to widely integrate epitaxial oxide devices based on FTJs, such as nonvolatile memories with different material platforms. For example, Lu et al.^[62] epitaxially grew an FTJ based on a 2.8 nm-thick BTO film on an STO substrate, released the FTJ device and transferred it onto an oxide-coated (SiO₂) Si(001) substrate. After that, arrays of circular Cu/Au electrodes were fabricated on top [Fig. 8c (left)]. The single crystallinity of the transferred BTO/LSMO/BTO trilayer was confirmed, and its electrical properties did not significantly decrease during transfer. A >100-fold difference in the tunnel current between the low-resistance state ('on' state, $\sim 200 \text{ nA}/\mu\text{m}^2$) and high-resistance state ('off' state, $\sim 0.5 \text{ nA}/\mu\text{m}^2$) was observed [Fig. 8c (right)], with all the key figures of merit showing good agreement with devices on oxide substrates. Luo et al.^[63] integrated centimeter-scale single-crystalline FTJs on flexible plastic substrates by water-etching-based epitaxial oxide membrane lift-off and subsequent transfer. The obtained flexible memristors, i.e., FTJs on plastic substrates, present high-speed and low-voltage-mediated memristive behaviors with resistance changes greater than 500% and are stable against shape changes. After that, the transfer of high-quality nanoscale epitaxial films of ferroelectric $\text{Ba}_{1-x}\text{Sr}_x\text{TiO}_3$ from single-crystal oxide substrates to silicon and polymer substrates without structural degradation was demonstrated,^[21] which provided an approach for the fabrication of ultrafast CMOS-compatible ferroelectric memories.

Energy harvesters can convert energy in the environment into electrical energy in various electronic devices^[101]. It is widely used in self-powering biomedical sensors, environmental monitors, and portable electronic devices. The flexibility brought about by the freestanding film pushes the

energy harvester one step closer to being wearable and implantable. When implanted in the human body, it can convert tiny movements such as heartbeats, diaphragm activities, and respiration movements into electrical signals^[102]. Using the LLO technique, the PZT film was lifted from the MgO and Al₂O₃ rigid substrate^[50]. Interdigitated electrodes (IDEs) with a finger length of 1.3 cm, an electrode width of 100 μm , an interelectrode gap of 100 μm , and 33 digitate pairs were fabricated on flexible PZT thin films, and the energy harvesters were coated with SU-8 photoresist with metal contact hole patterning. After that, poling processes were performed to produce remnant polarization in the PZT thin films. Fig. 8d displays the bending and unbending states of the flexible PZT energy harvester, and Fig. 8e shows that an open-circuit voltage of $\sim 250 \text{ V}$ and a short-circuit current of $\sim 2.3 \mu\text{A}$ were achieved on the flexible PZT thin-film energy harvester made from the MgO wafer. The current of the PZT energy harvester from MgO is more than two times greater than that of the PZT generator from Al₂O₃. Microvibration harvesters can serve as a complementary solution to conventional, bulky, and heavy electromagnetic devices. In addition, large-area PZT thin films on flexible substrates have also been studied^[103]. The LLO process was adopted to transfer a high-quality piezoelectric thin film from bulk sapphire substrates to plastic substrates, and eventually, a flexible piezoelectric energy harvesting device called a nanogenerator (NG) was fabricated. The PZT thin-film NG on a single thin plastic substrate exhibited a high output performance of $\sim 200 \text{ V}$ and $\sim 150 \mu\text{A}\cdot\text{cm}^{-2}$ from slight mechanical deformation, and the short-circuit current generated from a large-area NG ($3.5 \text{ cm} \times 3.5 \text{ cm}$) reached $\sim 8 \mu\text{A}$. Jeong et al.^[48] performed similar work on flexible PZT thin film-based energy harvesters and demonstrated a self-powered fully flexible light-emitting system enabled by a flexible energy harvester. In contrast, Hwang et al.^[104] used the solid-state single-crystal growth (SSCG) method for growing a flexible energy harvester enabled by a single-crystalline piezoelectric $(1-x)\text{Pb}(\text{Mg}_{1/3}\text{Nb}_{2/3})\text{O}_3 - (x)\text{Pb}(\text{Zr}, \text{Ti})\text{O}_3$ (PMN-PZT) thin film. A flexible interdigitated electrode (IDE)-type PMN-PZT harvester can generate an open-circuit voltage and short-circuit current of up to 100 V and 20 μA , respectively, through biomechanical bending and unbending motions.

6 Outlook

In recent years, the synthesis and integration of freestanding oxide films have been extensively studied, highlighting their immense potential for use in next-generation electronic/spintronics devices. However, the widespread adoption of oxide freestanding membranes in the near future is not anticipated. Next, we briefly discuss the opportunities and challenges in the research on freestanding oxide films.

First, freestanding oxide films can be integrated onto arbitrary substrates at room temperature, which differs from conventional methods for integrating materials with stable states under very different conditions. Theoretically, all epitaxial functional oxides as well as related structures, such as superlattices or multilayers, can be synthesized and transferred using release and transfer methods. Second,

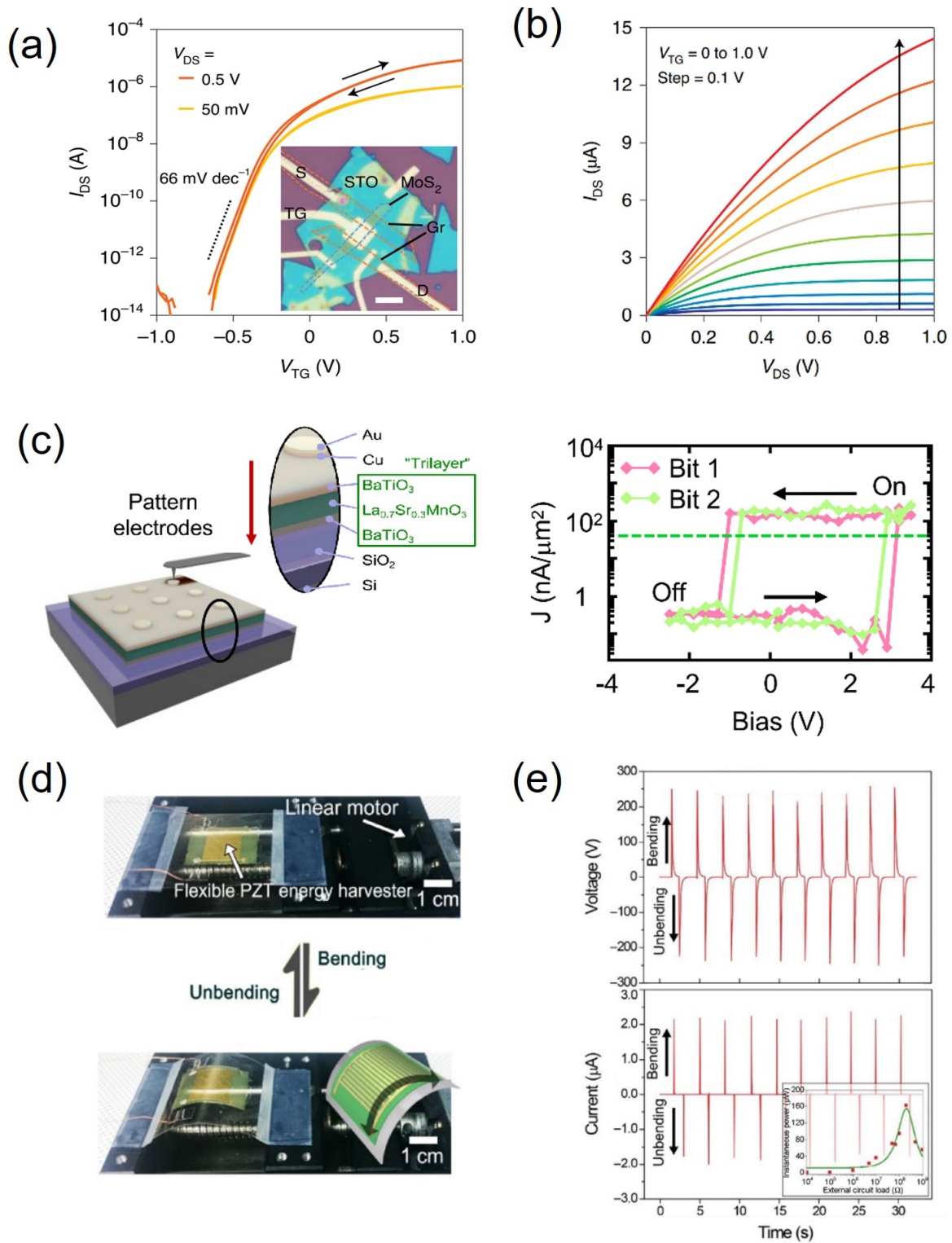


Fig. 8. (a,b) MoS₂ transistors with transferred STO top-gate dielectrics. (a) Double-sweep I_{DS} - V_{TG} characteristics of the device with the back gate grounded. The gate sweeping directions are indicated by the arrows. The inset shows an optical image of the device. The boundaries of graphene and MoS₂ are outlined by dashed lines. Scale bar, 10 μ m. (b) Output curves (I_{DS} - V_{DS}) with V_{TG} varying from 0 to 1.0 V at steps of 0.1 V. Reproduced with permission from Ref. [100]. Copyright 2022, Springer Nature. (c) Freestanding oxide FTJ memories transferred onto SiO₂-coated Si substrates (left). Tunnel current measured at 0.2 V DC voltage after a gradually increasing and decreasing pulsed bias showing characteristic hysteresis loops for two different junctions (right). Reproduced with permission from Ref. [62]. Copyright 2019, American Chemical Society. (d, e) Flexible energy harvester based on the freestanding PZT thin film. (d) Bending and unbending motions of flexible energy harvester devices by a linear motor. During mechanical stimulation, the voltage and current produced from (e) the flexible PZT thin-film generator made from the MgO wafer. Insets: instantaneous output power levels of the PZT thin-film energy harvester as a function of the external load resistance. Reproduced with permission from Ref. [50]. Copyright 2017, Springer Nature.

because of the lattice mismatch and interface oxidation, it is challenging to direct epitaxial oxide films on traditional semiconductor substrates (such as Si, Ge) to achieve integration. However, high-quality integration can be achieved through freestanding films. Third, freestanding films can achieve extraordinary one-dimensional/two-dimensional strains and strain gradients, which can greatly expand the exploration of phase diagram space and have the potential to reveal new materials and coupling mechanisms.

However, with respect to applications, the research progress is still in its infancy, as novel fabrication, release and transfer processes need to be further developed to take full advantage of these oxides. On the one hand, typical functional oxide materials are fragile and lack a slip system, which limits their application to both bendable and stretchable devices requiring a large bending state. On the other hand, compared with those of typical van der Waals materials, the crystallinity and integrity of freestanding oxide membranes remain unsatisfactory. Because of the strong electron correlation, such structural changes also lead to considerable degradation of the physical properties of freestanding oxide membranes, limiting their potential in next-generation electronic device applications. Moreover, handling these atomic membranes and heterogeneously integrating them onto other semiconductor platforms is an open challenge. These are also the key points for expanding the device application potential of freestanding oxides.

Acknowledgements

This work was supported by the Fundamental Research Funds for the Central Universities (WK9990000102, WK2030000035).

Conflict of interest

The authors declare that they have no conflict of interest.

Biographies

Ao Wang is a graduate student in the Hefei National Research Center for Physical Sciences at Microscale, University of Science and Technology of China. He received his B.S. degrees from Nankai University in 2022. His research interests focus on the preparation and characterization of freestanding oxide films.

Jinfeng Zhang is currently working as a postdoctor in the Hefei National Research Center for Physical Sciences at Microscale, University of Science and Technology of China (USTC). She received Ph.D. degrees from USTC, in 2024. She focuses on functional oxide thin film deposition and characterization and her main research interests include freestanding oxide films and flexible electronics based on functional oxides.

Lingfei Wang is a Professor at Hefei National Research Center for Physical Sciences at Microscale, University of Science and Technology of China (USTC). He received his Ph.D. degree in condensed-matter physics from USTC in 2013. From 2013 to 2015, he worked as a postdoctoral research associate at the King Abdullah University of Science and Technology, Saudi Arabia. From 2015 to 2020, he worked as a postdoctoral research associate and an assistant research professor at Seoul National University, Seoul. In 2020, he joined USTC as a professor. His research interests are focused on exploring the emergent interfa-

cial phenomena at the interfaces of correlated oxide heterostructures and developing oxide-based functional devices.

References

- [1] Reyren N, Thiel S, Cavaglia A D, et al. Superconducting interfaces between insulating oxides. *Science*, **2007**, *317*: 1196–1199.
- [2] Catalan G. Progress in perovskite nickelate research. *Phase Transitions*, **2008**, *81*: 729–749.
- [3] Catalan G, Scott J F. Physics and applications of bismuth ferrite. *Advanced Materials*, **2009**, *21*: 2463–2485.
- [4] Gao R, Jain A C P, Pandya S, et al. Designing optimal perovskite structure for high ionic conduction. *Advanced Materials*, **2020**, *32*: 1905178.
- [5] Salamon M B, Jaime M. The physics of manganites: Structure and transport. *Reviews of Modern Physics*, **2001**, *73*: 583–628.
- [6] Yu P, Chu Y H, Ramesh R. Oxide interfaces: Pathways to novel phenomena. *Materials Today*, **2012**, *15*: 320–327.
- [7] Jung I, Son J. A nonvolatile memory device made of a graphene nanoribbon and a multiferroic BiFeO₃ gate dielectric layer. *Carbon*, **2012**, *50*: 3854–3858.
- [8] Rajapitamahuni A, Hoffman J, Ahn C H, et al. Examining graphene field effect sensors for ferroelectric thin film studies. *Nano Letters*, **2013**, *13*: 4374–4379.
- [9] Aghabagheri S, Rasti M, Mohammadzadeh M, et al. High temperature superconducting YBCO microwave filters. *Physica C: Superconductivity and Its Applications*, **2018**, *549*: 22–26.
- [10] Wang S X, Chapline M G. Room-temperature spin filtering in a CoFe₂O₄/MgAl₂O₄/Fe₃O₄ magnetic tunnel barrier. *Physical Review B*, **2006**, *74* (1): 014418.
- [11] Liu W, Wang H. Flexible oxide epitaxial thin films for wearable electronics: Fabrication, physical properties, and applications. *Journal of Materiomics*, **2020**, *6*: 385–396.
- [12] Zhou Z, Trassin M, Gao Y, et al. Probing electric field control of magnetism using ferromagnetic resonance. *Nature Communications*, **2015**, *6*: 6082.
- [13] Zhao S, Li J, Cao D, et al. Recent advancements in flexible and stretchable electrodes for electromechanical sensors: Strategies, materials, and features. *ACS Applied Materials & Interfaces*, **2017**, *9*: 12147–12164.
- [14] Pesquera D, Fernández A, Khestanova E, et al. Freestanding complex-oxide membranes. *Journal of Physics: Condensed Matter*, **2022**, *34*: 383001.
- [15] Nelson C T, Gao P, Jokisaari J R, et al. Domain dynamics during ferroelectric switching. *Science*, **2011**, *334*: 968–971.
- [16] Zheng H, Wang J, Lofland S E, et al. Multiferroic BaTiO₃-CoFe₂O₄ nanostructures. *Science*, **2004**, *303*: 661–663.
- [17] Liu J, Feng Y, Tang R, et al. Mechanically tunable magnetic properties of flexible SrRuO₃ epitaxial thin films on mica substrates. *Advanced Electronic Materials*, **2018**, *4*: 1700522.
- [18] Jiang J, Bitla Y, Huang C W, et al. Flexible ferroelectric element based on van der Waals heteroepitaxy. *Science Advances*, **2017**, *3*: e1700121.
- [19] Li Y, Zhou P, Qi Y, et al. All-inorganic flexible high-temperature strain sensor based on SrRuO₃/muscovite heteroepitaxy. *Journal of the American Ceramic Society*, **2022**, *105*: 2038–2045.
- [20] Shen L, Wu L, Sheng Q, et al. Epitaxial lift-off of centimeter-scaled spinel ferrite oxide thin films for flexible electronics. *Advanced Materials*, **2017**, *29*: 1702411.
- [21] Pesquera D, Parsonnet E, Qualls A, et al. Beyond substrates: Strain engineering of ferroelectric membranes. *Advanced Materials*, **2020**, *32*: 2003780.
- [22] Lu D, Baek D J, Hong S S, et al. Synthesis of freestanding single-crystal perovskite films and heterostructures by etching of sacrificial water-soluble layers. *Nature Materials*, **2016**, *15*: 1255–1260.

- [23] Hong S S, Gu M, Verma M, et al. Extreme tensile strain states in $\text{La}_{0.7}\text{Ca}_{0.3}\text{MnO}_3$ membranes. *Science*, **2020**, 368: 71–76.
- [24] Dong G, Li S, Li T, et al. Periodic wrinkle-patterned single-crystalline ferroelectric oxide membranes with enhanced piezoelectricity. *Advanced Materials*, **2020**, 32: 2004477.
- [25] Dubnack O, Müller F A. Oxidic 2D materials. *Materials*, **2021**, 14: 5213.
- [26] Novoselov K S, Geim A K, Morozov S V, et al. Electric field effect in atomically thin carbon films. *Science*, **2004**, 306: 666–669.
- [27] Staley N E, Wu J, Eklund P, et al. Electric field effect on superconductivity in atomically thin flakes of NbSe_2 . *Physical Review B*, **2009**, 80: 184505.
- [28] Lake R, Zahid F. Thermoelectric properties of Quintuple Layer Bi_2Te_3 . *Applied Physics Letters*, **2010**, 97: 212102.
- [29] Wang X, You L X, Liu D K, et al. Thin-film-like BSCCO single crystals made by mechanical exfoliation. *Physica C Superconductivity*, **2012**, 474: 13–17.
- [30] Zeng M, Xiao Y, Liu J, et al. Exploring two-dimensional materials toward the next-generation circuits: From monomer design to assembly control. *Chemical Reviews*, **2018**, 118: 6236–6296.
- [31] Butler S Z, Hollen S M, Cao L, et al. Progress, challenges, and opportunities in two dimensional materials beyond graphene. *ACS Nano*, **2013**, 7: 2898–2926.
- [32] Utama M I B, de la Mata M, Magen C, et al. Twinning-, polytypism-, and polarity-induced morphological modulation in nonplanar nanostructures with van der Waals epitaxy. *Advanced Functional Materials*, **2013**, 23: 1636–1646.
- [33] Jaegermann W, Klein A, Pettenkofer C. Electronic properties of van der Waals-epitaxy films and interfaces. In: Hughes H P, Starnberg H I, editors. *Electron Spectroscopies Applied to Low-Dimensional Materials. Physics and Chemistry of Materials with Low-Dimensional Structures*. Netherlands, Dordrecht: Springer, **2000**, 317–402.
- [34] Bitla Y, Chu Y-H. MICAtronics: A new platform for flexible X-tronics. *FlatChem*, **2017**, 3: 26–42.
- [35] Ma C H, Lin J C, Liu H J, et al. Van der Waals epitaxy of functional MoO_2 film on mica for flexible electronics. *Applied Physics Letters*, **2016**, 108: 253104.
- [36] Liu H J, Wang C K, Su D, et al. Flexible heteroepitaxy of CoFe_2O_4 /muscovite bimorph with large magnetostriction. *ACS Applied Materials & Interfaces*, **2017**, 9: 7297–7304.
- [37] Chu Y H. Van der Waals oxide heteroepitaxy. *npj Quantum Materials*, **2017**, 2: 67.
- [38] Yang C, Han Y, Qian J, et al. Flexible, temperature-stable, and fatigue-endurable $\text{PbZr}_{0.52}\text{Ti}_{0.48}\text{O}_3$ ferroelectric film for nonvolatile memory. *Advanced Electronic Materials*, **2019**, 5: 1900443.
- [39] Bitla Y, Chen C, Lee H C, et al. Oxide heteroepitaxy for flexible optoelectronics. *ACS Applied Materials & Interfaces*, **2016**, 8: 32401–32407.
- [40] Li C I, Lin J C, Liu H J, et al. Van der Waal epitaxy of flexible and transparent VO_2 film on muscovite. *Chemistry of Materials*, **2016**, 28: 3914–3919.
- [41] Zhang C, Ding S, Qiao K, et al. Large low-field magnetoresistance (LFMR) effect in free-standing $\text{La}_{0.7}\text{Sr}_{0.3}\text{MnO}_3$ films. *ACS Applied Materials & Interfaces*, **2021**, 13: 28442–28450.
- [42] Kum H S, Lee H, Kim S, et al. Heterogeneous integration of single-crystalline complex-oxide membranes. *Nature*, **2020**, 578: 75–81.
- [43] Kum H, Lee D, Kong W, et al. Epitaxial growth and layer-transfer techniques for heterogeneous integration of materials for electronic and photonic devices. *Nature Electronics*, **2019**, 2: 439–450.
- [44] Kong W, Li H, Qiao K, et al. Polarity governs atomic interaction through two-dimensional materials. *Nature Materials*, **2018**, 17: 999–1004.
- [45] Wong W S, Sands T, Cheung N W. Damage-free separation of GaN thin films from sapphire substrates. *Applied Physics Letters*, **1998**, 72: 599–601.
- [46] Wu P C, Chu Y H. Development of oxide heteroepitaxy for soft technology. *Journal of Materials Chemistry C*, **2018**, 6: 6102–6117.
- [47] Tsakalakos L, Sands T. Epitaxial ferroelectric $(\text{Pb}, \text{La})(\text{Zr}, \text{Ti})\text{O}_3$ thin films on stainless steel by excimer laser liftoff. *Applied Physics Letters*, **2000**, 76: 227.
- [48] Jeong C K, Park K I, Son J H, et al. Self-powered fully-flexible light-emitting system enabled by flexible energy harvester. *Energy & Environmental Science*, **2014**, 7: 4035–4043.
- [49] Lee H S, Chung J, Hwang G T, et al. Flexible inorganic piezoelectric acoustic nanosensors for biomimetic artificial hair cells. *Advanced Functional Materials*, **2014**, 24: 6914–6921.
- [50] Jeong C K, Cho S B, Han J H, et al. Flexible highly-effective energy harvester via crystallographic and computational control of nanointerfacial morphotropic piezoelectric thin film. *Nano Research*, **2017**, 10: 437–455.
- [51] Zhang Y, Ma C, Lu X, et al. Recent progress on flexible inorganic single-crystalline functional oxide films for advanced electronics. *Materials Horizons*, **2019**, 6: 911–930.
- [52] Detchprohm T, Amano H, Hiramatsu K, et al. The growth of thick GaN film on sapphire substrate by using ZnO buffer layer. *Journal of Crystal Growth*, **1993**, 128: 384–390. DOI: 10.1016/0022-0248(93)90353-X
- [53] Yablonovitch E, Gmitter T, Harbison J P, et al. Extreme selectivity in the lift-off of epitaxial GaAs films. *Applied Physics Letters*, **1987**, 51: 2222–2224.
- [54] Paskiewicz D M, Sichel-Tissot R, Karapetrova E, et al. Single-crystalline SrRuO_3 nanomembranes: A platform for flexible oxide electronics. *Nano Letters*, **2016**, 16: 534–542.
- [55] Zhang Y, Shen L, Liu M, et al. Flexible quasi-two-dimensional CoFe_2O_4 epitaxial thin films for continuous strain tuning of magnetic properties. *ACS Nano*, **2017**, 11: 8002–8009.
- [56] Bakaul S R, Serrao C R, Lee M, et al. Single crystal functional oxides on silicon. *Nature Communications*, **2016**, 7: 10547.
- [57] Bakaul S R, Serrao C R, Lee O, et al. High speed epitaxial perovskite memory on flexible substrates. *Advanced Materials*, **2017**, 29: 1605699.
- [58] Gan Q, Rao R A, Eom C B, et al. Direct measurement of strain effects on magnetic and electrical properties of epitaxial SrRuO_3 thin films. *Applied Physics Letters*, **1998**, 72: 978–980.
- [59] Qi Y, Jafferis N T, Lyons K Jr, et al. Piezoelectric ribbons printed onto rubber for flexible energy conversion. *Nano Letters*, **2010**, 10: 524–528.
- [60] Qi Y, Kim J, Nguyen T D, et al. Enhanced piezoelectricity and stretchability in energy harvesting devices fabricated from buckled PZT ribbons. *Nano Letters*, **2011**, 11: 1331–1336.
- [61] Baek D J, Lu D, Hikita Y, et al. Mapping cation diffusion through lattice defects in epitaxial oxide thin films on the water-soluble buffer layer $\text{Sr}_3\text{Al}_2\text{O}_6$ using atomic resolution electron microscopy. *APL Materials*, **2017**, 5: 096108.
- [62] Lu D, Crossley S, Xu R, et al. Freestanding oxide ferroelectric tunnel junction memories transferred onto silicon. *Nano Letters*, **2019**, 19: 3999–4003.
- [63] Luo Z D, Peters J J P, Sanchez A M, et al. Flexible memristors based on single-crystalline ferroelectric tunnel junctions. *ACS Applied Materials & Interfaces*, **2019**, 11: 23313–23319.
- [64] Wang H, Shen L, Duan T, et al. Integration of both invariable and tunable microwave magnetisms in a single flexible $\text{La}_{0.67}\text{Sr}_{0.33}\text{MnO}_3$ thin film. *ACS Applied Materials & Interfaces*, **2019**, 11: 22677–22683.
- [65] Chen Z, Wang B Y, Goodge B H, et al. Freestanding crystalline $\text{YBa}_2\text{Cu}_3\text{O}_{7-x}$ heterostructure membranes. *Physical Review Materials*, **2019**, 3: 060801.
- [66] Gu K, Katayama T, Yasui S, et al. Simple method to obtain large-size single-crystalline oxide sheets. *Advanced Functional Materials*, **2020**, 30: 2001236.

- [67] Wang Q, Fang H, Wang D, et al. Towards a large-area freestanding single-crystal ferroelectric BaTiO₃ membrane. *Crystals*, **2020**, *10* (9): 733.
- [68] Zhang B, Yun C, MacManus-Driscoll J L. High yield transfer of clean large-area epitaxial oxide thin films. *Nano-Micro Letters*, **2021**, *13*: 39.
- [69] Kim D, Jung W K, Lee S. Single-crystalline-level properties of ultrathin SrRuO₃ flexible membranes with wide and clean surface. *njp. Flexible Electronics*, **2022**, *6*: 24.
- [70] Hong S S, Yu J H, Lu D, et al. Two-dimensional limit of crystalline order in perovskite membrane films. *Science Advances*, **2017**, *3*: eaao5173.
- [71] Ji D, Cai S, Paudel T R, et al. Freestanding crystalline oxide perovskites down to the monolayer limit. *Nature*, **2019**, *570*: 87–90.
- [72] Singh P, Swartz A, Lu D, et al. Large-area crystalline BaSnO₃ membranes with high electron mobilities. *ACS Applied Electronic Materials*, **2019**, *1*: 1269–1274.
- [73] Xu R, Huang J, Barnard E S, et al. Strain-induced room-temperature ferroelectricity in SrTiO₃ membranes. *Nature Communications*, **2020**, *11*: 3141.
- [74] Zhang J, Lin T, Wang A, et al. Super-tetragonal Sr₄Al₂O₇ as a sacrificial layer for high-integrity freestanding oxide membranes. *Science*, **2024**, *383*: 388–394.
- [75] Li D, Adamo C, Wang B Y, et al. Stabilization of Sr₃Al₂O₆ growth templates for *ex situ* synthesis of freestanding crystalline oxide membranes. *Nano Letters*, **2021**, *21*: 4454–4460.
- [76] Suk J W, Kitt A, Magnuson C W, et al. Transfer of CVD-grown monolayer graphene onto arbitrary substrates. *ACS Nano*, **2011**, *5*: 6916–6924.
- [77] Lu Z, Liu J, Feng J, et al. Synthesis of single-crystal La_{0.67}Sr_{0.33}MnO₃ freestanding films with different crystal-orientation. *APL Materials*, **2020**, *8*: 051105.
- [78] Chen X D, Liu Z B, Zheng C Y, et al. High-quality and efficient transfer of large-area graphene films onto different substrates. *Carbon*, **2013**, *56*: 271–278.
- [79] Keimer B, Kivelson S A, Norman M R, et al. From quantum matter to high-temperature superconductivity in copper oxides. *Nature*, **2015**, *518*: 179–186.
- [80] Hwang H Y, Iwasa Y, Kawasaki M, et al. Emergent phenomena at oxide interfaces. *Nature Materials*, **2012**, *11*: 103–113.
- [81] Khan Y, Obaidulla S M, Habib M R, et al. Recent breakthroughs in two-dimensional van der Waals magnetic materials and emerging applications. *Nano Today*, **2020**, *34*: 100902.
- [82] Harbola V, Crossley S, Hong S S, et al. Strain gradient elasticity in SrTiO₃ membranes: Bending versus stretching. *Nano Letters*, **2021**, *21*: 2470–2475.
- [83] Davidovikj D, Groenendijk D J, Monteiro A M R V L, et al. Ultrathin complex oxide nanomechanical resonators. *Communications Physics*, **2020**, *3*: 163.
- [84] Dai L, Zhao J, Li J, et al. Highly heterogeneous epitaxy of flexoelectric BaTiO_{3-δ} membrane on Ge. *Nature Communications*, **2022**, *13*: 2990.
- [85] Guo R, You L, Lin W, et al. Continuously controllable photoconductance in freestanding BiFeO₃ by the macroscopic flexoelectric effect. *Nature Communications*, **2020**, *11*: 2571.
- [86] Cai S, Lun Y, Ji D, et al. Enhanced polarization and abnormal flexural deformation in bent freestanding perovskite oxides. *Nature Communications*, **2022**, *13*: 5116.
- [87] Huang J, Wang H, Sun X, et al. Multifunctional La_{0.67}Sr_{0.33}MnO₃ (LSMO) thin films integrated on mica substrates toward flexible spintronics and electronics. *ACS Applied Materials & Interfaces*, **2018**, *10*: 42698–42705.
- [88] Dong G, Li S, Yao M, et al. Super-elastic ferroelectric single-crystal membrane with continuous electric dipole rotation. *Science*, **2019**, *366*: 475–479.
- [89] Peng B, Peng R C, Zhang Y Q, et al. Phase transition enhanced superior elasticity in freestanding single-crystalline multiferroic BiFeO₃ membranes. *Science Advances*, **2020**, *6*: eaba5847.
- [90] Jin C, Zhu Y, Li X, et al. Super-flexible freestanding BiMnO₃ membranes with stable ferroelectricity and ferromagnetism. *Advanced Science*, **2021**, *8*: 2102178.
- [91] An F, Qu K, Zhong G, et al. Highly flexible and twistable freestanding single crystalline magnetite film with robust magnetism. *Advanced Functional Materials*, **2020**, *30*: 2003495.
- [92] Elangovan H, Barzilay M, Seremi S, et al. Giant superelastic piezoelectricity in flexible ferroelectric BaTiO₃ membranes. *ACS Nano*, **2020**, *14*: 5053–5060.
- [93] Wu P C, Wei C C, Zhong Q, et al. Twisted oxide lateral homostructures with conjunction tunability. *Nature Communications*, **2022**, *13*: 2565.
- [94] Chen S, Zhang Q, Rong D, et al. Braiding lateral morphotropic grain boundaries in homogenetic oxides. *Advanced Materials*, **2023**, *35*: 2206961.
- [95] Han L, Addiego C, Prokhorenko S, et al. High-density switchable skyrmion-like polar nanodomains integrated on silicon. *Nature*, **2022**, *603*: 63–67.
- [96] Li Y, Zatterin E, Conroy M, et al. Electrostatically driven polarization flop and strain-induced curvature in free-standing ferroelectric superlattices. *Advanced Materials*, **2022**, *34*: 2106826.
- [97] Dubourdieu C, Bruley J, Arruda T M, et al. Erratum: Switching of ferroelectric polarization in epitaxial BaTiO₃ films on silicon without a conducting bottom electrode. *Nature Nanotechnology*, **2013**, *8*: 881.
- [98] Warusawithana M P, Cen C, Sleasman C R, et al. A ferroelectric oxide made directly on silicon. *Science*, **2009**, *324*: 367–370.
- [99] Yao M, Cheng Y, Zhou Z, et al. Recent progress on the fabrication and applications of flexible ferroelectric devices. *Journal of Materials Chemistry C*, **2020**, *8*: 14–27.
- [100] Yang A J, Han K, Huang K, et al. Van der Waals integration of high-κ perovskite oxides and two-dimensional semiconductors. *Nature Electronics*, **2022**, *5*: 233–240.
- [101] Wang Z, Pan X, He Y, et al. Piezoelectric nanowires in energy harvesting applications. *Advances in Materials Science and Engineering*, **2015**, *2015*: 165631.
- [102] Wang Z L, Wu W. Nanotechnology-enabled energy harvesting for self-powered micro-/ nanosystems. *Angewandte Chemie International Edition*, **2012**, *51*: 11700–11721.
- [103] Park K I, Son J H, Hwang G T, et al. Highly-efficient, flexible piezoelectric PZT thin film nanogenerator on plastic substrates. *Advanced Materials*, **2014**, *26*: 2514–2520.
- [104] Hwang G T, Yang J, Yang S H, et al. A reconfigurable rectified flexible energy harvester via solid-state single crystal grown PMN–PZT. *Advanced Energy Materials*, **2015**, *5*: 1500051.